*Tellus* (1990), *42A*, 3–13

# Cyclogenesis and frontogenesis

By W. R. PELTIER, G. W. KENT MOORE and S. POLAVARAPU, *Department of Physics, University of Toronto, Toronto, Ontario, Canada M5S 1A7*

(Manuscript received 31 October 1988; in final form 4 April 1989)

ABSTRACT

Detailed linear analysis of the stability of realistic atmospheric frontal structures using the full hydrostatic primitive equations has demonstrated that such localized baroclinic zones support instability at two distinct and well-separated length scales, even when the frontal mean states have uniform potential vorticity. The first scale is associated with the well-known Charney-Eady mode of baroclinic instability with a wavelength of 3000–4000 km that is responsible for the generation of observed mid-tropospheric long waves. The second scale is defined by an apparently new mode of baroclinic instability, that we have previously called the "cyclone mode", which has a wavelength near 1000 km and is boundary confined rather than being troposphere filling as is the case of the Charney-Eady mode. The most important characteristic of the cyclone mode is that it is completely filtered by both the quasi-geostrophic and semi-geostrophic approximations to the equations of motion. In this paper, we demonstrate explicitly through the analysis of a specific case of polar low development that this new mode is an important actor in at least one recurrent atmospheric dynamical process. Besides reviewing and extending these linear stability analyses, we describe a number of rather interesting results that we have obtained from a new series of *f*-plane analyses of the non-linear life cycles of frontal baroclinic waves. These have already provided considerable new insight into the detailed dynamics of the processes through which frontal waves "break".

## 1. Introduction

The conventional interpretation of all mid-latitude cyclones is that they are manifestations of the baroclinic instability mechanism first described by Charney (1947) and Eady (1949) based upon the quasi-geostrophic approximation to the equations of motion. Although Charney (1975) clearly recognized that there was some fundamental dynamical difference between the upper level long waves that quasi-geostrophic theory so successfully describes, and the shorter wavelength frontal cyclones upon which Bjerknes (1919) had focussed his attention, no clear theoretical explanation supporting the necessity of such distinction has been forthcoming until recently.

In Moore and Peltier (1987), we described a detailed analysis of the stability of realistic atmospheric frontal structures against arbitrary three dimensional perturbations. The frontal structures employed in this initial investigation were those generated by the action of a hyperbolic deformation field on a previously existing large-scale horizontal potential temperature gradient. The semi-geostrophic theory of Eliassen (1948) and Hoskins and Bretherton (1972) was employed to describe the process of frontogenesis. The frontal zones generated in this way, for which the assumption of uniform potential vorticity was also employed, were used as basic states for the purpose of the stability analysis. In this analysis the quasi-geostrophic approximation was not invoked and the complete non-separable eigenvalue problem was solved without approximation. The main result obtained from this work was the demonstration of the existence of a second branch of unstable normal modes in the eigen-spectrum, in addition to the long-wave branch that contains the classical Charney-Eady mode. The fastest growing mode in the short wave branch was found to have a horizontal wavelength somewhat less than 1000 km, in close accord with the observed scale of frontal cyclones (Bjerknes and Solberg, 1922; Harrold and Browning, 1969; Reed, 1979). An analysis of the energy budget for the new cyclone scale mode demonstrated that it was also driven by the baroclinic instability mechanism.

The relationship between this new mode of baroclinic instability and the classical Charney-Eady mode has been the subject of a number of recent further investigations, the main results of which will be discussed here. The most important of these (Moore and Peltier, 1989a) has been the demonstration that the quasi-geostrophic approximation completely filters the new mode from the dynamical system while leaving the Charney-Eady mode only slightly affected. This can be understood on the basis of the fact that the short wavelength mode in the primitive equations system is boundary confined and therefore is excluded from the spectrum of a constant potential vorticity basic state by the Charney-Stern Theorem of quasi-geostrophic theory. When semi-geostrophic theory is employed in the stability analysis (Moore and Peltier, 1989b), we find that it is similarly incapable of supporting the new short wavelength cyclone mechanism, as we will further illustrate here, although this slight improvement on quasi-geostrophic theory does deliver an essentially exact facsimile of the Charney-Eady modes in the primitive-equations system, fully correcting the small errors in this branch that were clearly evidenced in the quasi-geostrophic analysis.

There are several further questions that are posed by the discovery of the new cyclone scale mode of baroclinic instability that is supported by the primitive equations system. Firstly, we must demonstrate that it does play a crucial role in the generation of observed cyclone scale disturbances such as polar lows and comma clouds. Secondly, we must enquire whether the relatively large linear growth rate of the new mode is always an accurate guide to its ability to develop to significant amplitude and thereby to affect appreciable mean flow modification. To this end we have begun a new series of baroclinic wave life cycle experiments using a nonhydrostatic anelastic numerical model in which the individual experiments are initialized with the eigenfunctions of the fastest growing modes of Charney-Eady and cyclone scale baroclinic instability. Initial results that have been obtained concerning some of these further questions will be briefly summarized.

## 2. Non-separable baroclinic instability and frontal cyclogenesis

The problem of frontal instability as we will formulate it here is basically as follows. Given a zonal flow $V(x, z)$ in thermal wind balance with a background potential temperature field $\theta(x, z)$, viz:

$$f\frac{\partial V}{\partial z} = \frac{g}{\theta_0}\frac{\partial \theta}{\partial x}, \tag{1}$$

determine the stability of this structure against arbitrary three dimensional fluctuations. In writing (1) in this form we have employed the pseudo-height of Hoskins and Bretherton (1972) as vertical coordinate. The characteristic structures in whose stability we are interested are structures such as that illustrated in Fig. 1 which shows a typical model front, in this case one generated by the action of a hyperbolic deformation field upon a pre-existing tan-hyperbolic variation of potential temperation using the semi-geostrophic theory of Hoskins and Bretherton (1972). The stability of such structures may be analysed using a number of different approximations to the complete set of hydrodynamic field equations. Even if the class of perturbations is restricted to those that are hydrostatic, there nevertheless remain a number of such levels of approximation, e.g., full primitive equations, semi-geostrophic theory, quasi-geostrophic theory, etc. But no matter what level of approximation is employed to perform the stability analysis the central mathematical problem involves the solution of a nonseparable, two dimensional boundary value problem whose associated boundary conditions involve the eigenvalue itself. Over the past several years we have solved a number of such problems that arise in atmospheric dynamics applications (Klaassen and Peltier, 1985; Moore and Peltier, 1987; Laprise and Peltier, 1989) by making use of ideas from Floquet theory, e.g., Jordan and Smith (1977). We simply assume that the basic state $(V, \theta)$ to be perturbed is extended onto a lattice periodic in $x$. It then follows from the imposed $x$-periodicity of

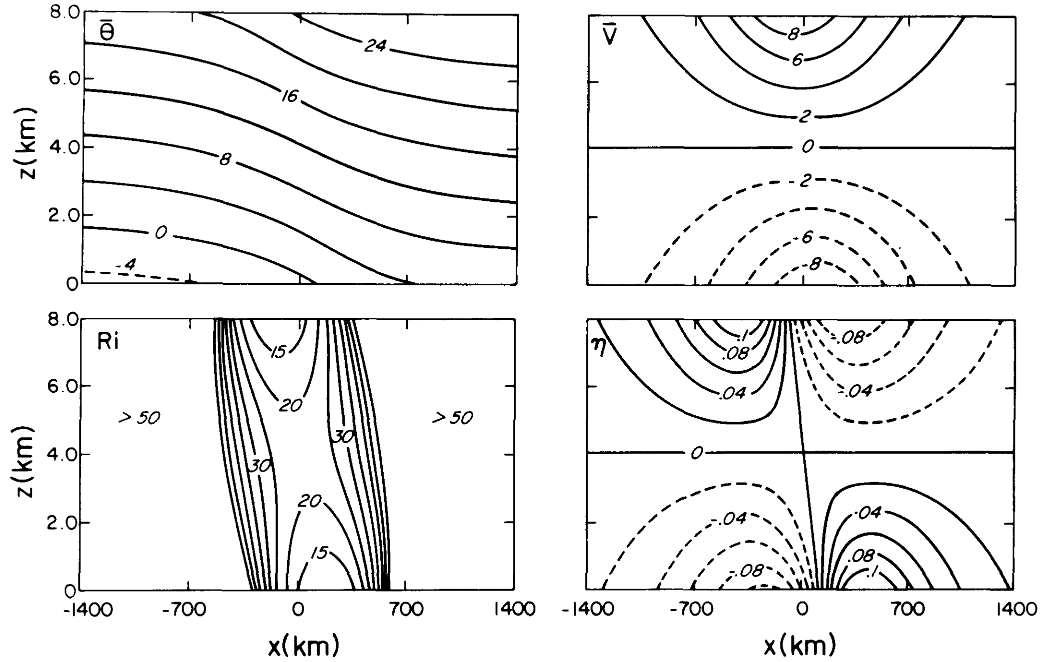


*Fig. 1.* Typical constant potential vorticity Hoskins-Bretherton frontal zone represented by the fields of potential temperature, along front velocity, Richardson number and vorticity.

the basic state that the normal modes of the set of linear stability equations governing the fate of small amplitude fluctuations have the following form:

$$F(x, y, z; t) = \mathrm{Re}[F^{\dagger}(x, z)\, e^{i(ax+by)+st}], \tag{2a}$$

$$F^{\dagger}(x, z) = F^{\dagger}(x, +4L, z), \tag{2b}$$

with $4L$ the basic $x$-periodicity of the lattice and $F$ representing any of the hydrodynamic fields that enter the stability analysis at the level of approximation in question. We will very briefly discuss the results obtained from three such levels of approximation here, using the front shown on Fig. 1 as basic state in each case.

### *2.1. Frontal cyclogenesis using the primitive equations*

Substituting expansions of the form (2) for each of the hydrodynamic fields into the full non-hydrostatic primitive equations yields the set of stability equations (Moore and Peltier 1987):

$$su^{\dagger} + ibVu^{\dagger} - (f/\alpha_0)^2 v^{\dagger} + (f/\alpha_0)^2 (\partial/\partial_x + ia)\phi^{\dagger} = 0, \tag{3a}$$

$$sv^{\dagger} + ibVv^{\dagger} + D^{\dagger} V + u^{\dagger} + ib\phi^{\dagger} = 0, \tag{3b}$$

$$sw^{\dagger} + ibw^{\dagger} + (N/\alpha_0)^2 \theta^{\dagger} + (N/\alpha_0)^2 \partial\phi^{\dagger}/\partial z = 0, \tag{3c}$$

$$s\theta^{\dagger} + ibV\theta^{\dagger} + D^{\dagger}\Theta = 0, \tag{3d}$$

$$(\partial/\partial_x + ia)u^{\dagger} + ibv^{\dagger} + \partial w^{\dagger}/\partial z = 0, \tag{3e}$$

$$L\phi^{\dagger} = (f/\alpha_0)^2 ((\partial/\partial_x + ia)v^{\dagger} - ibu^{\dagger}) + (N/\alpha_0)^2 \partial\theta^{\dagger}/\partial z - 2\left(ib\,\partial/\partial_x \overline{V}u^{\dagger} + ib\frac{\partial\overline{V}}{\partial z} w^{\dagger}\right). \tag{3f}$$

In this system, the operators $D^{\dagger}$ and $L$ are defined as follows:

$$D^{\dagger} = u^{\dagger}\,\partial/\partial x + w^{\dagger}\,\partial/\partial z, \tag{4a}$$

$$L = (f/\alpha_0)^2 (\partial/\partial x + ia)^2 - b^2 + (N/\alpha_0)^2 \partial^2/\partial z^2, \tag{4b}$$

and the other symbols have their conventional hydrodynamic meanings. Subject to the hydrostatic approximation and using Galerkin representations for each of the unknown fields, the above system may be reduced to a standard matrix eigenvalue problem which has the complex growth rate $s$ as eigenvalue (see Moore and

Peltier 1987 for details). From the associated eigenfunctions one may compute the various correlations that contribute to the energy budgets of the modes and thereby gain understanding of the processes that give rise to their growth.

Fig. 2 shows typical growth rate versus along-front wavenumber spectra for a family of fronts of the form shown on Fig. 1 that differ only in their across front contrast in potential temperature. The predominant feature of these spectra is that they are characterized by the presence of two distinct local maxima in growth rate, one corresponding to a wavelength near 4000 km and another to a wavelength near 1000 km. Analysis in Moore and Peltier (1987) showed these waves to be troposphere filling analogues of Charney-Eady waves and boundary confined (i.e., shallow) disturbances respectively. Because the frontal mean state in which these instabilities occur is one of constant potential vorticity, the short wavelength boundary confined modes are possible only because the full primitive hydrostatic system has been employed in the stability analysis. In the absence of cross-front gradients of potential vorticity (Bretherton, 1966) the

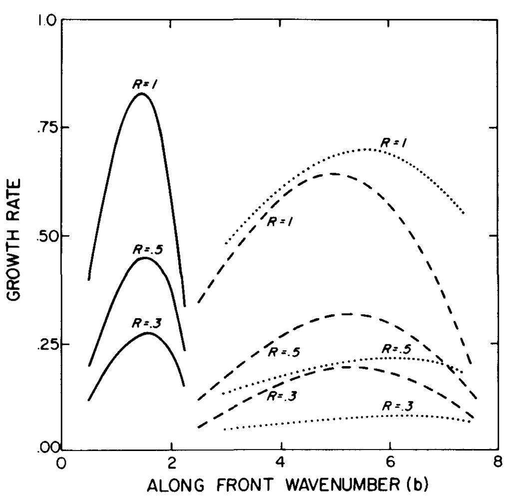


*Fig. 2.* Phase speed and growth rate versus along-front wavenumber spectra for Hoskins-Bretherton frontal zones such as that shown in Fig. 1 as a function of the non-dimensional across-front temperature contrast $R$. $R = 1$ corresponds to a 12°C contrast. In this and all subsequent Figures the along-front wavenumber is non-dimensionalized with a length scale of 800 km that equals the Rossby radius of deformation.

Charney-Stern (1963) Theorem of quasigeostrophic theory demonstrates that the boundary confined branch of short wavelength modes could not exist. What of an intermediate theory such as the semi-geostrophic theory of Hoskins and Bretherton (1972)?

### 2.2. *Frontal cyclogenesis using the geostrophic momentum approximation*

The basis of the geostrophic momentum approximation (Eliassen, 1948; Hoskins, 1975) is that Lagrangian parcel accelerations are assumed small compared to the Coriolis force which leads to replacement of the horizontal momentum vector by its geostrophic equivalent. The effect of the advection of the geostrophic wind by the ageostrophic wind is thereby retained, an effect that is excluded in quasi-geostrophic theory. In this theory the stability of a frontal mean state such as that shown in Fig. 1 is governed by the following single p.d.e. for the perturbation geopotential $\phi'$ (Hoskins, 1975):

$$\left[\frac{\partial}{\partial T} + \bar{V}\frac{\partial}{\partial Y}\right]\left[\frac{1}{f^2}\left[\frac{\partial^2 \phi'}{\partial X^2} + \frac{\partial^2 \phi'}{\partial Y^2}\right] + \frac{f}{Q}\frac{\partial^2 \phi'}{\partial Z^2}\right] = 0, \tag{5a}$$

with boundary conditions

$$\left[\frac{\partial}{\partial T} + \bar{V}\frac{\partial}{\partial Y}\right]\frac{\partial \phi'}{\partial z} - \frac{g}{f\theta_0}\frac{\partial \bar{\Theta}}{\partial X}\frac{\partial \phi'}{\partial Y} = 0 \tag{5b}$$

on $Z = 0$ and $Z = H$. In this system, the independent variables are:

$$X = M/f = x + \bar{V}/f; \; Y = y; \; Z = z; \quad \text{and} \quad T = t,$$

with $M = fx + \bar{V}$ the angular momentum field and $(x, y, z, t)$ the usual Cartesian co-ordinates. A numerical method suitable for the solution of (5) has been described in detail in Moore and Peltier (1989b). As in the primitive equations analysis discussed above, we seek solutions of the Floquet form:

$$\phi'(x, y, z, T) = \mathrm{Re}[\phi^{\dagger}(x, z)\,e^{i(aX + bY) + sT}]. \tag{6}$$

Phase speed ($\mathrm{Im}\, s/b$) and growth rate ($\mathrm{Re}\, s$) spectra for semi-geostrophic stability of the front shown on Fig. 1 are presented in Fig. 3 where they are compared to results obtained from the PE analyses discussed above and the QG analysis to be discussed below. Comparing Fig. 3 (in which the modes all have Floquet parameter $a = 0$) with Fig. 2, we note that the main

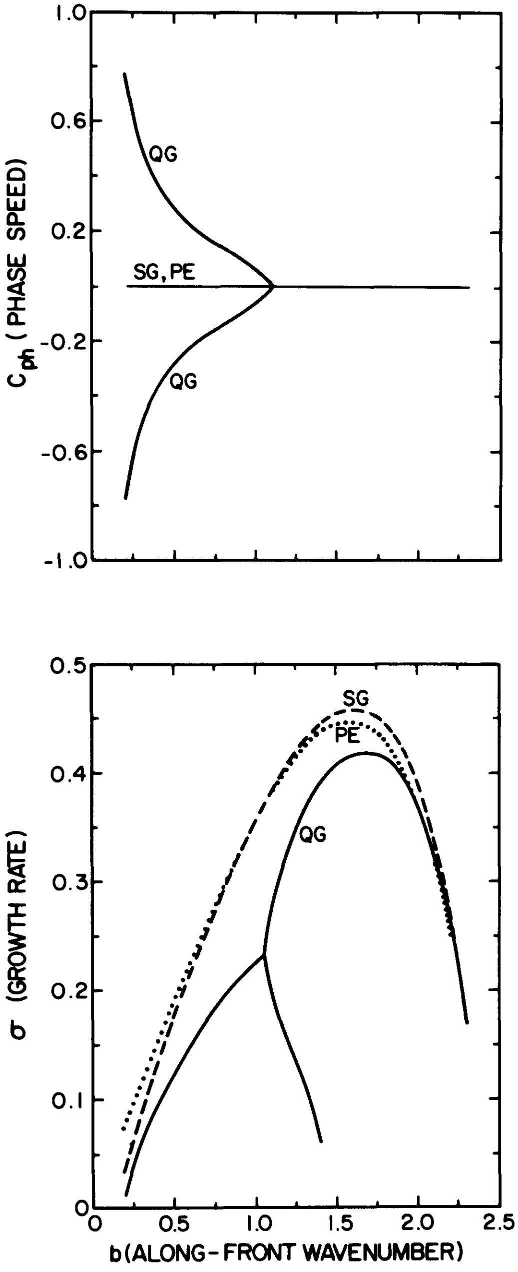


*Fig. 3.* Phase speed and growth rate versus along front wavenumber spectra for semi-geostrophic (SG) and quasi-geostrophic (QG) theories compared with the corresponding primitive equations (PE) result from Fig. 2. The short-wave branch of unstable modes is entirely absent in the results of both SG and QG theory.

difference between the PE and SG spectra is the absence of the cyclone scale mode from the SG result. This short wavelength branch has been completely filtered by the semi-geostrophic approximation. However the phase speed and growth rate versus wavenumber spectra are virtually identical with those delivered by the full primitive equations analysis for long wavelength (Charney-Eady) waves. How these results compare with those obtained using quasi-geostrophic theory, a theory with an even lower order of accuracy, is discussed in Subsection 2.3.

### 2.3. *Frontal cyclogenesis using quasi-geostrophic theory*

In the quasi-geostrophic approximation, the stability equation that replaces (5) is the usual equation for the conservation of potential vorticity, which, expressed in terms of the quasi-geostrophic perturbation geopotential $\phi'_g$ is:

$$\left[\frac{\partial}{\partial t}+\bar{V}\frac{\partial}{\partial y}\right]\left[\frac{\partial^2\phi'_g}{\partial x^2}+\frac{\partial^2\phi'_g}{\partial y^2}+\frac{f^2}{N^2}\frac{\partial^2\phi'_g}{\partial z^2}\right] = \frac{\partial\bar{q}}{\partial x}\frac{\partial\phi'_g}{\partial y}, \tag{7}$$

with

$$\left[\frac{\partial}{\partial t}+\bar{V}\frac{\partial}{\partial y}\right]\frac{\partial\phi'_g}{\partial z} = \frac{\partial}{\partial z}\bar{V}\frac{\partial}{\partial y}\phi'_g \quad \text{on } z=0, H,$$

in which $N^2=(g/\theta_0)\,\partial\Theta/\partial z$ is the square of the Brunt-Väisälä frequency (assumed $x$-independent in quasi-geostrophic theory) and $\partial\bar{q}/\partial x$ is the cross-front gradient of potential vorticity, $\partial\bar{q}/\partial x = \partial^2\bar{V}/\partial x^2 + f^2\,\partial/\partial z[N^{-2}\,\partial\bar{V}/\partial z]$, a term that is clearly zero for constant potential vorticity frontal zones such as that illustrated in Fig. 1 as was assumed above in writing (5). When (7) is employed to analyse the stability of the front shown in Fig. 1, the phase speed and growth rate versus along front wavenumber spectra obtained (see Moore and Peltier, 1989a for details) are those shown on the previously discussed Fig. 3 where they are marked QG to distinguish them from the results obtained with the primitive equations (PE) and with semi-geostrophic (SG) theory. Inspection of the QG results on Fig. 3 for the Charney-Eady branch shows them to be very much more complicated than the results obtained with either of the more accurate theories. The $\sigma$ versus $b$ and $C_{ph}$ versus $b$ curves for the QG waves split into distinct branches at small $b$ (long wavelength), where both modes have the same growth rate but different phase speeds, one slightly faster and one slightly slower than the zero phase speed that characterizes the Charney-Eady waves delivered by both PE and SG theory. The reason for this complexity in the QG spectra is discussed in detail in Moore and Peltier (1989b) and is associated with the fact that the Charney-Eady wave may be understood as a couplet of phase locked edge waves nucleated on the upper and lower rigid surfaces (e.g., Gill, 1982). The members of the QG couplet interact along lines of constant $x$ whereas those of the equivalent SG couplet interact along lines of constant $X = x + \overline{V}/f$. Because the axis of maximum baroclinicity is very nearly parallel to lines of constant $X$, the modes in the SG analysis are able to track this variation efficiently whereas the QG waves are not. The fact that the long waves in the PE analysis are essentially identical to the SG waves demonstrates that the SG analysis correctly embodies the most important dynamical effects found in the more accurate PE model.

The most important *result* revealed by this brief sequence of comparisons, however, is that neither the SG nor the QG approximations are able to account for the appearance of the "cyclone branch" of unstable modes revealed by the PE analysis of the stability of frontal zones characterized by constant potential vorticity. The important *issue* of course is whether or not this new mode of baroclinic instability has anything to do with recurrent atmospheric phenomenology. We believe it does. Specifically we suggest that it may be the mechanism responsible for the nucleation of polar front cyclones, polar lows, and comma clouds. One specific example which appears to verify the truth of this conjecture is discussed in the next section.

## 3. The genesis of a polar low wavetrain

Fig. 4a shows the cross sections of along front velocity and potential temperature fields that were observed by Reed and Duncan (1987) to characterize the mean atmospheric state through which a train of distinct cyclonic disturbances was observed to propagate. The Richardson number field

$$\mathrm{Ri} = \frac{g}{\theta_0} \frac{\partial\overline{\theta}/\partial z}{(\partial\overline{V}/\partial z)^2}, \tag{8a}$$

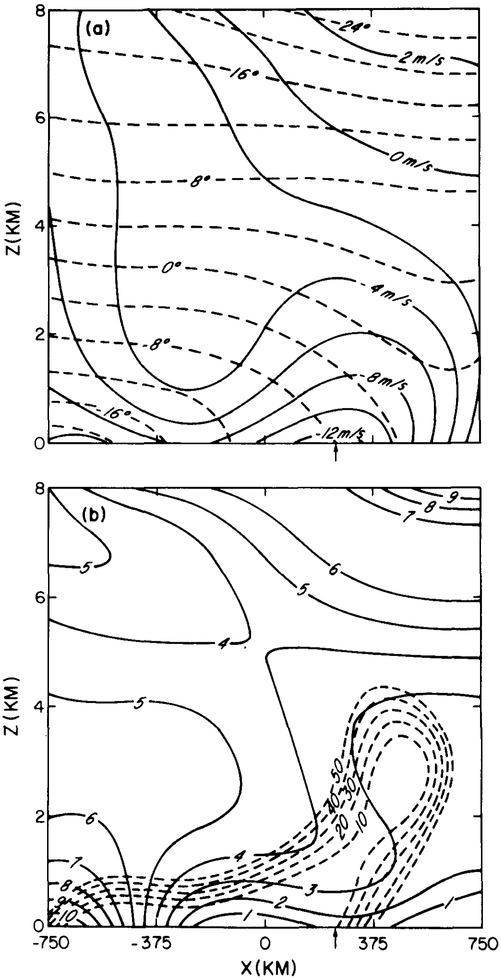


*Fig. 4.* (a) Cross-sections of potential temperature and along-front velocity representing the basic state in which the polar low wave train of Reed and Duncan (1987) was observed. (b) Cross-sections of static stability (solid lines °C/km) and Richardson number (dashed lines) derived from the fields shown in (a). The arrow at the bottom of each plot indicates the location in which the polar lows were observed to develop.

and the static stability field

$$S = \partial\overline{\theta}/\partial z, \tag{8b}$$

associated with this atmospheric state are displayed in Fig. 4b. The arrow indicates the location of the storm track of the lows. From this figure, it is clear that the wavetrain nucleated in a region in which both the Richardson number and static stability were small. The wavelength of the observed baroclinic waves was very near 500 km and they formed over the North Atlantic between Greenland to the west and Northwestern Europe to the east. In Fig. 5, we show the phase speed and growth rate versus along front wavenumber spectra predicted by our primitive equations theory when it is applied to determine the stability of the cross sections shown in Fig. 4. Inspection of these spectra shows them to reveal two distinct instability maxima, one corresponding to the Charney-Eady scale near 4000 km and the second corresponding to the observed cyclone scale of 500 km. Unlike the corresponding spectra for the constant potential vorticity frontal zone shown in Fig. 2, in which the long-wave and short-wave branches had comparable growth rates, for this observed polar low wavetrain the theory predicts that the cyclone scale mode should be much more vigorous than the Charney-Eady mode. Not only does the new theory correctly predict the observed dominance of the cyclone scale disturbance but it also correctly predicts the doubling time of wave amplitude that was inferred by Reed and Duncan to be about 6 hours. The results for our PE theory shown in Fig. 5 correspond to a predicted doubling time of almost precisely the observed. This result rather strongly argues that the genesis and rapid development of such disturbances need not involve strong feedback with moist convective processes except insofar as these processes may be important in determining the mean state of the environment in which development occurs, specifically the region of low static stability near the surface that turns out to be an important feature of regions in which the cyclone scale mode can grow efficiently according to our theory. Our analysis of this example is completed by Fig. 6 in which we show the eigenfunctions of the fastest growing cyclone mode in terms of Reynolds stress (RS) and the vertical and horizontal heat flux correlations (VHF and HHF, respectively). Mathematical forms for these correlations are given explicitly in Moore and Peltier (1987). Our purpose in showing these results for the cyclone mode is to compare the observed position of the storm track, which we show on the plate labelled VHF as a vertically pointing arrow on the abscissa, with the position of the maximum of horizontal and vertical heat flux. Inspection shows that the correlation is essentially perfect, further reinforcing the validity of our theory. The energy box diagram in the lower left of this Figure demonstrates the manner in which these correlations contribute to the growth of the mode and mark it as a conventional baroclinic instability, at least with respect to its energetics.

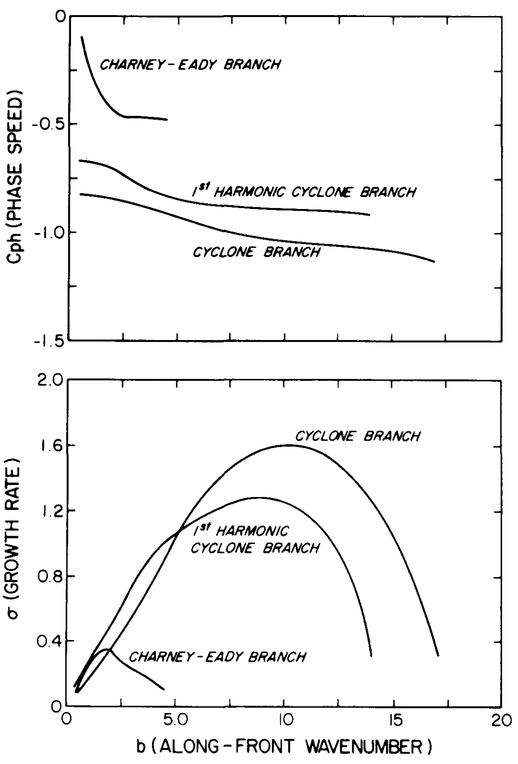


*Fig. 5.* Non-dimensional phase speed ($C_{ph}$) and growth rate ($\sigma$) versus along-front wavenumber (b) spectra for the basic state shown in Fig. 4. The phase speeds, growth rates and wavenumbers have been scaled by 8 m/s, $10^{-5}$ s$^{-1}$ and $1.25 \times 10^{-6}$ m$^{-1}$ respectively.

## 4. The nonlinear evolution of frontal cyclones

Even though the linear analyses briefly reviewed above are strongly suggestive of the importance of the new cyclone scale mode of baroclinic instability that we have shown to be supported by primitive equations dynamics, a number of questions clearly remain, among

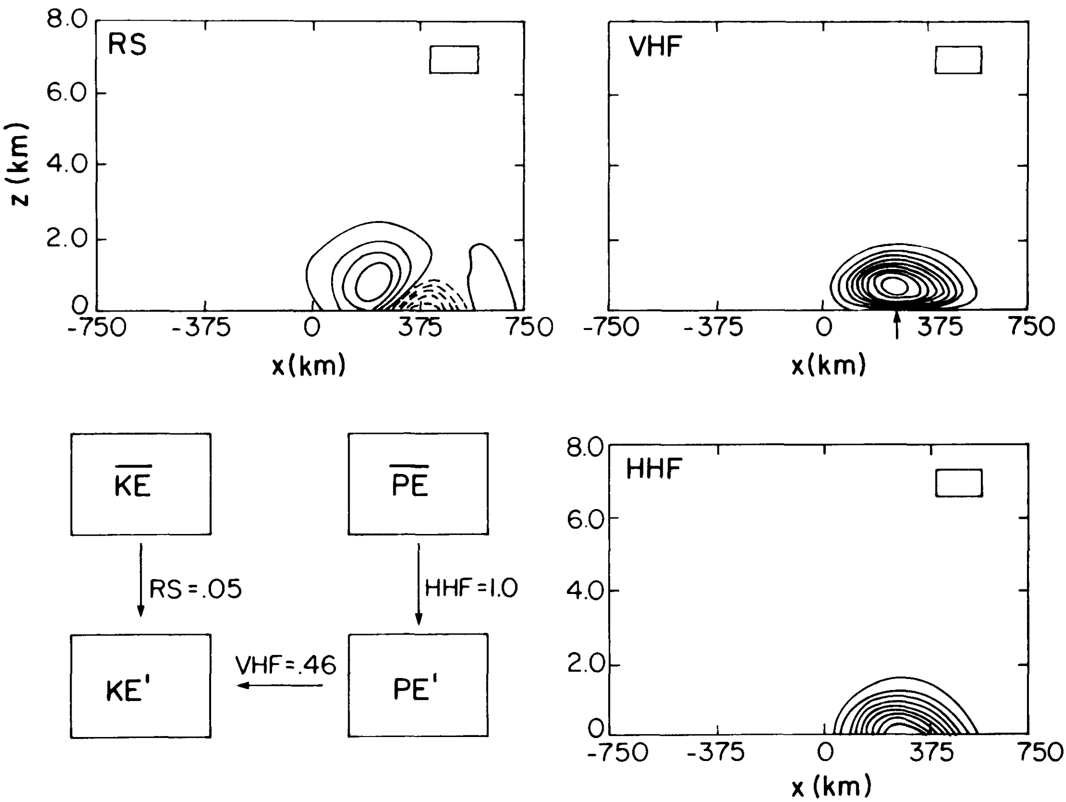


*Fig. 6.* Contributions to the energy budget of the growing cyclone wave due to the Reynolds stress (RS), and vertical and horizontal (VHF and HHF) heat flux correlations respectively. The correlations contribute to the transfer of energy from mean state potential ($\overline{PE}$) and kinetic ($\overline{KE}$) energy to the energy of the perturbation in the manner represented on the standard energy box diagram shown in the lower left hand corner of the Figure. Detailed mathematical expressions for the correlations are provided in Moore and Peltier (1987).

which are many concerning the ability of the cyclone scale mode to achieve significant amplitude. We might also be interested to know whether the new mode might naturally appear as a secondary phase of development in the life cycle (and along the "fronts") of a longer wavelength Charney-Eady mode as suggested in Moore and Peltier (1987). In concluding this brief summary of ongoing research in our group at Toronto we will focus briefly upon the latter issue by way of illustrating the further results that will be forthcoming shortly from this program.

We have been employing the same three-dimensional non-hydrostatic anelastic model described in Clark (1977), and employed by Peltier and Clark (1979, 1983) in previous analyses of the mechanics of nonlinear mountain waves, to follow the evolution of the baroclinic waves generated by the Charney-Eady and cyclone scale modes of frontal instability into the nonlinear regime. Here, we shall focus on the life-cycle of the long wave that develops on the same frontal structure shown in Fig. 1 whose stability was previously described. The single integration that we will discuss was performed on an $f$-plane in a channel of height $H = 8$ km, length $L = 3142$ km, and width $W = 4700$ km and 17, 63, and 95 grid points were employed to resolve the fields in each of these respective spatial co-ordinate directions. The integration was performed on the recently installed CRAY X-MP at the University of Toronto and used 1.6 MW of main memory.

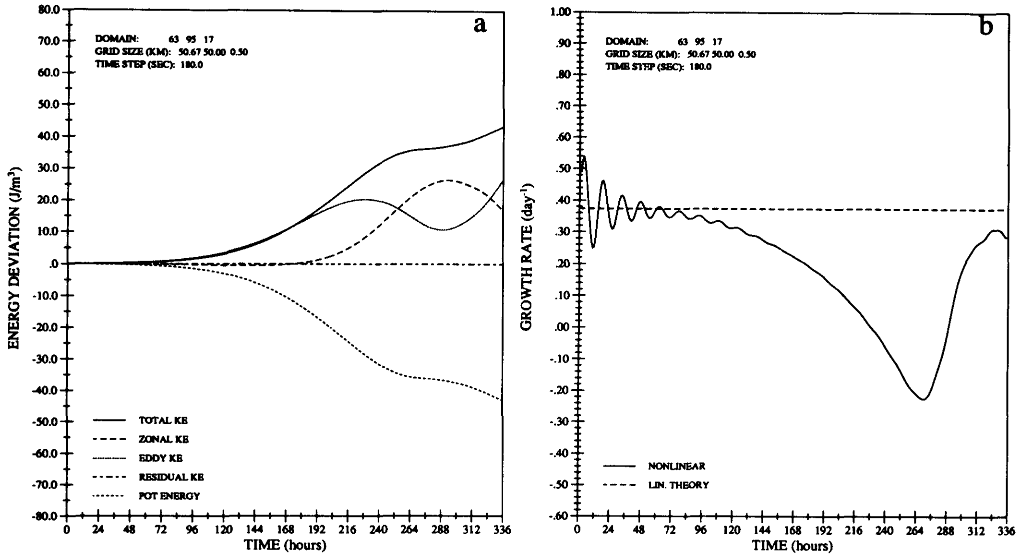


*Fig. 7.* (a) Histories of wave energy evolution for the Charney-Eady wave on the mean state shown in Fig. 1. (b) Comparison of the growth rate history for perturbation kinetic energy from the nonlinear simulation with the prediction of linear stability theory (dashed line).

The 14 day integration to be described required 7 h of CPU time to complete and employed an inviscid version of the code with the normally employed first order closure for the eddy diffusion and the time filters suppressed. A summary of the life cycle of the baroclinic wave according to this computation is provided in Fig. 7a where the evolution with time of the individual components of the wave energy are shown for the full 14-day period. Even in this highly compressed summary of the nonlinear wave life cycle we may discern a number of interesting features. Foremost among these is probably the fact, which is clear from the history of perturbation kinetic energy, that the amplitude of the wave does not decay monotonically to zero following its rise to maximum. Rather the wave appears to enter a regime which is characterized by a limit cycle behaviour of the perturbation kinetic energy as was shown to be the case in previous analyses of the nonlinear life cycles of Kelvin-Helmholtz waves (Peltier et al., 1978; Davis and Peltier, 1979; Klaassen and Peltier, 1985). In Fig. 7b, we show the variation with time of the growth rate of the wave, computed from 0.5 d ln $KE'/dt$, and compare it (dashed line) to the growth rate predicted using the linear stability theory sketched in Subsection 2.1 above. In the nonlinear integration, the growth-rate initially oscillates with large but decreasing amplitude about the linear prediction. This is due to the excitation of an inertial oscillation by the start-up procedure that we employed. This decays quite rapidly however, as the wave enters the finite amplitude regime in which it is able to effect significant mean flow modification. That the nonlinear model delivers such an accurate fit to the linear prediction of the growth rate of the frontal wave is very useful confirmation of the validity of both analyses.

The actual structure of the nonlinear wave at a sequence of times through its life-cycle is illustrated in Fig. 8 by planforms of the potential temperature field on the lower boundary of the model domain. Initially, the wave has the sinusoidal along-front structure predicted by linear stability theory. As it grows it develops a highly nonlinear form, however, and eventually "occludes" as the central region of low pressure and cyclonic winds "cuts-off" in the way that has been well described by synopticians. An extremely interesting characteristic of the flows that obtain late in the life cycle of the baroclinic wave, as described by these almost-inviscid experiments, is that they are characterized by a multiplicity of distinctly separate fronts (in the last frame of Fig. 8, three such secondary "fronts" exist over about $\frac{2}{3}$ of the length of the model domain). It would therefore appear that the formation of multiple-fronts, observations of which have been made (Reed, 1979; Shapiro and Keyser, 1988), may be a natural outcome of the nonlinear growth of synoptic scale waves on the mid-latitude polar front. Another interesting feature of the non-linear integration that is associated with the formation of multiple fronts is the development of warm and cold cores. These cores are separated from the primary warm and cold air masses by the secondary fronts. This shedding process is highly reminiscent of what is observed to occur to the ring-like structures that develop along the Gulf Stream (Wood, 1988). We also note that there is no evidence in this initial life-cycle simulation of the formation of cyclone scale disturbances along the fronts of the growing Charney-Eady wave.

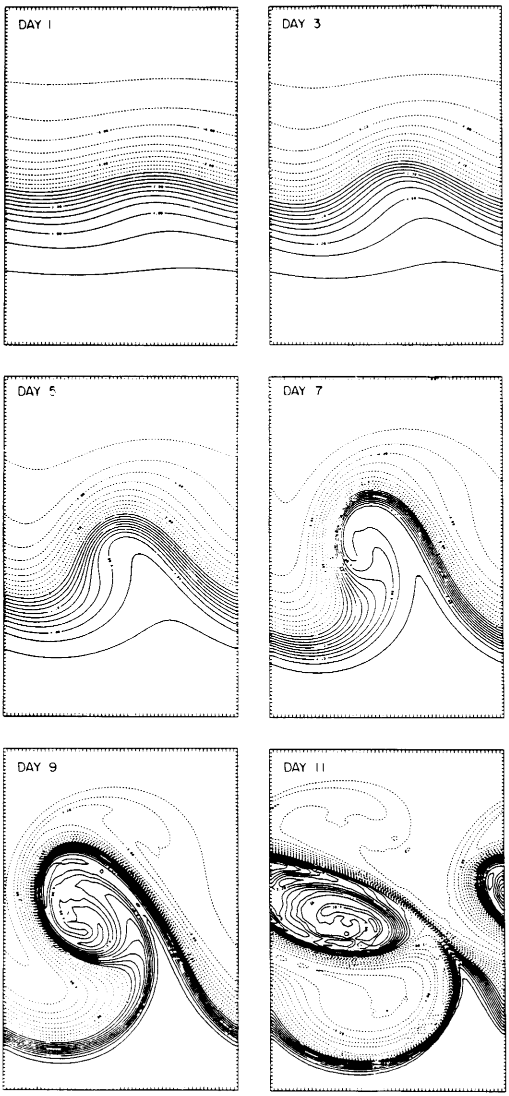


*Fig. 8.* Plan views of the evolving potential temperature field from the anelastic Charney-Eady wave simulation on the 1 km level and at 2 day intervals. Note the formation of the cut-off low pressure pool of warm air that forms as the wave "breaks".

## 5. Conclusions

We have briefly summarized results that have been obtained over the last few years in the course of a new program on the nature of mid-latitude cyclogenesis that has been undertaken by the atmospheric dynamics group in the Department of Physics at the University of Toronto. The main result so far obtained in this program has been the demonstration of the existence of a new cyclone scale mode of frontal baroclinic instability that requires the full dynamics of the hydrostatic primitive equations for its release. This mode appears to offer a very straightforward explanation for phenomena as diverse as polar front cyclones, Baiu front cyclones, polar lows, and comma clouds. We are currently investigating the nonlinear life cycles of such baroclinic waves using an anelastic nonhydrostatic model. This aspect of the program has already delivered interesting new insights into the processes that may be responsible for the formation of multiple fronts and Gulf Stream ring formation. One of the most interesting problems that we shall be able to address in the near future that is made possible by our use of a nonhydrostatic model to investigate the evolution of baroclinic waves, is the very important issue of the feedback of cumulous convection onto the long wave. Because the model that we employ has a two-way interactive nesting capability, given sufficient computational resources, we will eventually be able to explicitly resolve the cumulous dynamics that develop within the baroclinic wave and to describe the evolution of the coupled system.

## REFERENCES


Bjerknes, J. 1919. On the structure of moving cyclones. *Geofys. Publ. 1* (2).

Bjerknes, J. and Solberg, H. 1922. Life cycle of cyclones and the polar front theory of atmospheric circulation. *Geofys. Publ. 3* (1).

Bretherton, F. P. 1966. Baroclinic instability and the short wavelength cut-off in terms of potential vorticity. *Quart. J. Roy. Met. Soc. 92*, 335–345.

Charney, J. G. 1947. The dynamics of long waves in a baroclinic westerly current. *J. Meteor. 4*, 135–162.

Charney, J. G. 1975. Selected papers of J. A. Bjerknes, *Western Periodicals.*

Charney, J. G. and Stern, M. E. 1963. On the stability of internal baroclinic waves in a rotating atmosphere. *J. Atmos. Sci. 19*, 159–172.

Clark, T. L. 1977. A small scale dynamical model using a terrain following co-ordinate transformation. *J. Comp. Phys. 24*, 186–215.

Davis, P. A. and Peltier, W. R. 1979. Some characteristics of the Kelvin-Helmholtz and resonant over-reflection modes of shear flow instability and of their interaction through vortex pairing. *J. Atmos. Sci. 36*, 2394–2412.

Eady, E. T. 1949. Long waves and cyclone waves. *Tellus 1*, 33–52.

Eliassen, E. 1948. The quasi-static equations of motion. *Geofys. Publ. 17* (3).

Gill, A. E. 1982. *Atmosphere-ocean dynamics*, Academic Press, 662 pp.

Harrold, T. W. and Browning, K. A. 1969. The polar low as a baroclinic disturbance. *Quart. J. Roy. Meteor. Soc. 95*, 710–723.

Hoskins, B. J. 1975. The geostrophic momentum approximation and the semi-geostrophic equations. *J. Atmos. Sci. 32*, 233–242.

Hoskins, B. J. and Bretherton, F. P. 1972: Atmospheric frontogenesis: mathematical formulation and solution. *J. Atmos. Sci. 29*, 11–37.

Jordan, D. W. and Smith, P. 1977. *Non-linear ordinary differential equations.* Oxford University Press.

Klaassen, G. P. and Peltier, W. R. 1985. The onset of turbulence in finite amplitude Kelvin-Helmholtz billows. *J. Fluid Mech. 155*, 1–35.

Laprise, R. P. and Peltier, W. R. 1989. The linear stability of nonlinear mountain waves: implications for the understanding of severe downslope windstorms. *J. Atmos. Sci. 46*, 545–564.

Moore, G. W. K. and Peltier, W. R. 1987: Cyclogenesis in frontal zones. *J. Atmos. Sci. 44*, 384–409.

Moore, G. W. K. and Peltier, W. R. 1989a. Non-separable baroclinic instability. Part I: Quasi-geostrophic dynamics. *J. Atmos. Sci. 46*, 57–78.

Moore, G. W. K. and Peltier, W. R. 1989b. Frontal cyclogenesis and the geostrophic momentum approximation. *Geophys. Astrophys. Fluid Dyn. 45*, 183–197.

Peltier, W. R. and Clark, T. L. 1979. The evolution and stability of finite amplitude mountain waves. Part II: Surface wave drag and severe downslope windstorms. *J. Atmos. Sci. 36*, 1498–1529.

Peltier, W. R. and Clark, T. L. 1983: Nonlinear mountain waves in two and three spatial dimensions. *Quart. J. Roy. Meteor. Soc. 109*, 527–548.

Peltier, W. R., Halle, J. and Clark, T. L. 1978. The evolution of finite amplitude Kelvin-Helmholtz billows. *Geophys. Astrophys. Fluid Dyn. 10*, 53–87.

Reed, R. J. 1979. Cyclogenesis in polar air streams. *Mon. Wea. Rev. 107*, 38–52.

Reed, R. J. and Duncan, C. N. 1987. Baroclinic instability as a mechanism for the serial development of polar lows: a case study. *Tellus 39A*, 376–384.

Shapiro, M. A. and Keyser, D. 1988. On the structure and dynamics of fronts, jet streams and the tropopause. *Palmén Memorial Symposium on Extratropical Cyclones. Amer. Meteor. Soc.* 177–181.

Wood, R. 1988. Unstable waves on oceanic fronts: Large amplitude behaviour and mean flow generation. *J. Phys. Ocean. 18*, 775–787.